

A Hybrid Visualization of the Environment using Smart Ultrasound-based Sensor Arrays

Emir Sokic, Kenan Softic, Mina Ferizbegovic, Jasmina Zubaca and Melita Ahic-Djokic

Faculty of Electrical Engineering, Sarajevo, Bosnia and Herzegovina

Keywords: Sensory System, Environment Analysis, Distributed System, Ultrasound, Laser, Sensor, Robotics.

Abstract: This paper presents the work in progress on the design and testing of a distributed ultrasound-based sensory system for hybrid 1D and 2D environment visualisation. Many common sensors used in robotics, such as infrared and ultrasonic sensors, cameras and lasers mainly focus on quantifying distances and shapes, while rarely have the ability to differentiate among different sensed surfaces/materials. We propose an inexpensive prototype sensory system based on popular ultrasonic sensors which uses ultrasonic reflections to determine the acoustic reflection coefficients. This additional feature allows differentiating among sensed objects. Moreover, the developed ultrasonic cells are equipped with a microcontroller for basic signal processing and a communication link for integration into a sensor network. In this paper, we discuss the possibility of fusing obtained sensor array data and laser measurements.

1 INTRODUCTION

Probably the most important part of an autonomous robotic system is a precise and reliable sensing element. Without sensors, it is extremely difficult to achieve any type of motion control. Techniques such as SLAM (simultaneous localization and mapping problem) rely on information provided by sensors (Fuentes-Pacheco et al., 2015). Analysis of the robotic system surroundings is very important in different areas: industrial robotics (Kaltsoukalas et al., 2015), medical surgery, space exploration (Elfes et al., 2006), and autonomous navigation of unmanned underwater, ground, or air vehicle, just to name a few.

Different types of sensors are used for environment analysis: infrared and ultrasonic sensors, (thermal) cameras, lasers etc. Different sensors have different disadvantages: optical sensors are sensitive to environmental conditions (such as light, rain, fog, etc.) (Benet et al., 2002), lasers are power-demanding (Jung et al., 2008) and expensive, RGB cameras cannot provide information about distance of nearby objects or object structure on their own (Fernández et al., 2007).

In contrast, ultrasonic sensors are cheap, relatively accurate and reliable. These sensors, which are widely used in robotic systems, flow measurements (Han et al., 2011), fault detection (D. Champaigne,

2007) and process monitoring (Kim et al., 2011) are able to assess the structure and solidity of materials (Grzelak et al., 2014).

Common low-cost solutions, such as the popular HC-SR04, are ultrasonic sensors primarily developed for distance measurements. In our previous work (Zubaca et al., 2015) we have described the design of an ultrasonic cell which is able to measure the distance and additionally measure the magnitude of the reflected ultrasonic wave and differentiate among different materials. In this paper we will briefly present the ultrasonic cell, while more information may be found in (Zubaca et al., 2015).

A single ultrasonic cell may be used as a standalone sensing element. However, using multiple spatially distributed sensors may enrich the information on the observed environment. Therefore, we proposed and developed a sensor array/network. The ultrasonic cells communicate on two different buses: SPI bus used for automatic remote (re)programming of the cells, and RS485 bus for communication. The buses are controlled by a master device, which acts as the in-between element that processes communication between slave ultrasonic cells and master PC computer.

One of the final goals of this project is to create a hybrid multidimensional sensing platform, as illustrated in Figure 1. Combining ultrasonic readings with other sensors (e.g. RGB camera) enables ac-

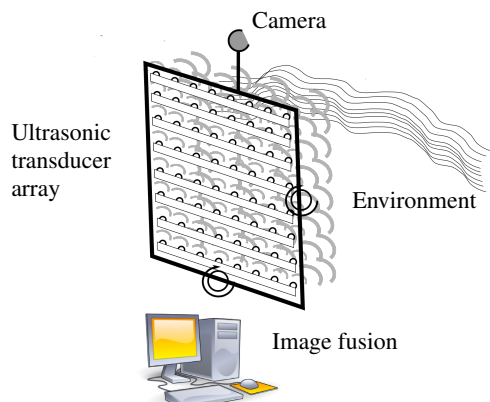


Figure 1: The hybrid 2D imaging system - ultrasonic cells and RGB camera. Sensor array is mounted on a platform with optional two degrees of freedom for an improved spatial coverage.



Figure 2: Left: original RGB image, Right: the expected structural image (different materials are represented by different gray levels).

quiring a multidimensional informationally-rich image. Every single cell analyses a smaller visual angle, while an array creates a hybrid image for a wider spatial area. Ideally, using the proposed system one may obtain images shown in Figure 2. Therefore, objects with different structure/surface may be represented by different attributes (e.g. grayscale intensity), which is the ultimate goal of this research.

Since this paper represents the work in progress, it is focused on the implementation of 1D array of ultrasonic cells, which allows obtaining plane maps of surroundings. Moreover, we have compared and validated the system measurement results with laser measurements, and presented a method for data fusion. The RGB image fusion are considered to be the part of a future work.

The paper is organized as follows. Section II describes the principles of operation of the ultrasonic cell. A brief report on the current hardware and software organization of the measurement system is given in Section III, while the experimental results are presented in the last section, together with conclusions and guidelines for future work.

2 PRINCIPLE OF OPERATION

Ultrasonic waves emitted from a sound source propagate through the air and when they reach an obstacle they will reflect back. The time needed for the sound wave to travel forward and backward can be easily measured. Under the assumption that the sound speed is constant, the distance between the source and obstacle is simply computed knowing the time-of-flight. This is the general principle used for distance measurement (e.g. HC-SR04 sensor).

The reflected sound wave is attenuated due to two facts: attenuation of sound waves due to the absorption in air, and due to the absorption of the obstacle itself. Therefore, if the distance from the obstacle is known, then it is possible to determine its acoustic reflection coefficient. In other words, two different obstacles at a same distance will reflect sound waves with different magnitudes.

As derived in the paper (Zubaca et al., 2015), a simplified sound propagation model may be described using:

$$A_r = \underbrace{A_0}_{\text{initial flight}} \cdot e^{-\alpha d} \cdot \underbrace{R}_{\text{reflection}} \cdot e^{-\alpha d}, \quad (1)$$

$$= A_0 \cdot R \cdot e^{-2\alpha d}, \quad (2)$$

$$= A_0 \cdot R \cdot 10^{-B \cdot 2 \cdot d / 10}, \quad (3)$$

$$\Rightarrow R = \frac{A_r}{A_0} 10^{B \cdot 2 \cdot d / 10}, \quad (4)$$

where A_r and A_0 represents the magnitudes of the reflected and transmitted waves respectively, R is the reflection coefficient of the material, d is the distance between the obstacle and the ultrasonic sensor, while $B = 10\alpha$ represents the attenuation of the ultrasonic wave in the air, which includes the losses induced by voltage-sound conversion, temperature, pressure and humidity (Vladišauskas and Jakevičius, 2004).

3 SYSTEM DESIGN

The proposed distributed system consists of three parts: array of ultrasonic cells, master device and communication controller and a master processing software on a PC.

3.1 Smart Sensor - Ultrasonic Cell

A block-structure of the developed ultrasonic cell is provided in Figure 3, while its physical realisation is given in Figure 4. The ultrasonic cell is based around an Atmel ATmega328p controller and the UTT4016 ultrasonic transceiver.

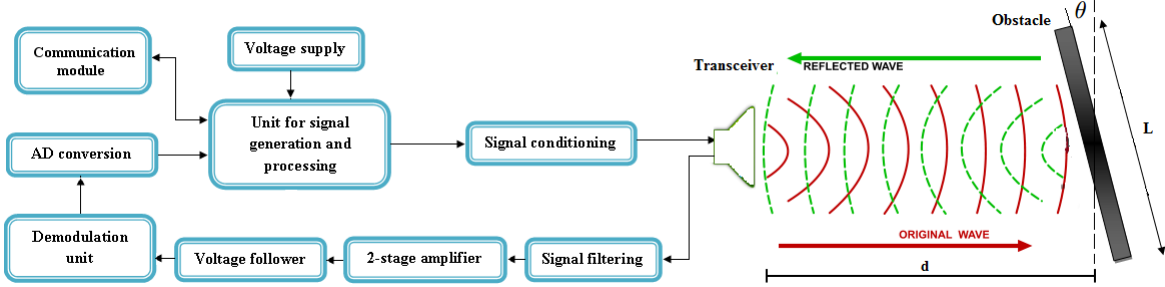


Figure 3: Ultrasonic cell structure.

The MCU is used for exciting the transceiver, simple preprocessing of received sound signals and establishing communication between a master PC and the ultrasonic transceiver.

The transceiver sends and receives ultrasound on 40kHz central frequency.

The master PC sends requests to the MCU over a RS485 bus to generate square wave signals, typically bursts with duration of 0.5ms. These bursts are converted to sine waves using band-pass filtering properties of the ultrasonic transceiver. Then, sinusoidal waves are emitted from the transceiver, and received back. Signal filtering and amplification is conducted on the board. In order not to violate the Nyquist-Shannon theorem related to the maximal MCU AD converter signal sampling rate (6kHz), the amplified voltage signals with central frequency 40kHz are demodulated to the [0 – 2kHz] band. The MCU samples and processes the demodulated signal with 6kHz sampling rate, estimates the magnitude of the reflected signal, and sends it back to the PC in real-time. The estimation is based on truncated Whittaker-Shannon-Kotelnikov series (Ye and Song, 2012):

$$U_D(t) = \sum_{k=-N}^N U_S(kT) \text{sinc}(2\omega_C(t - kT)), \quad (5)$$

where $\text{sinc}(t) = \sin t / t$ for $t \neq 0$ and $\text{sinc}(0) = 1$, $2N + 1$ represents the number of samples, T is the sampling period, and ω_C is the band-limit of the demodulated signal. Our setup used $N = 50$ samples, which resulted in the maximal error of 5.6% over the full scale range. Typical on-board signals are presented in Figure 5.

Experimentally obtained mapping of the reflection coefficients for some common materials/objects is presented in Figure 6 (from (Zubaca et al., 2015)).

3.2 Master Controller and Communication Module

The master controller and communication module is designed to be an interface between the PC and re-



Figure 4: Physical implementation of the ultrasonic cell. The dimensions of the cell are 5x5 [cm], with the possibility of reducing the dimensions to 2.5x5 [cm] by cutting and stacking the two segments of the PCB on top of each other.

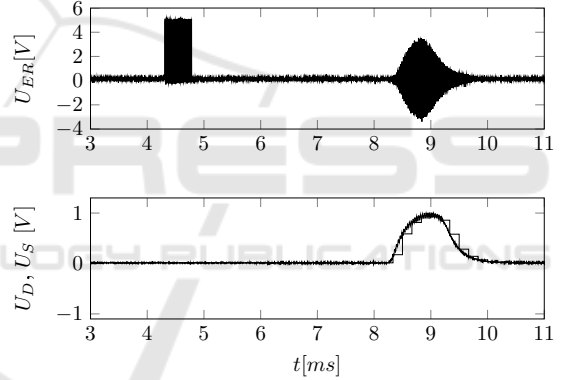


Figure 5: Signals generated and received by the transceiver (U_{ER}), the demodulated signal (U_D) and discrete-time sampled demodulated signal (U_S) processed by the MCU.

mote ultrasonic cells. It consists of a master controller and communication bus. The structure of the proposed system is depicted in Figure 7.

The master controller is essentially an Atmel ATmega2560 microcontroller which is primarily used to activate slave select (SS) pins and provide SPI functionality to a remote PC during cell programming. It

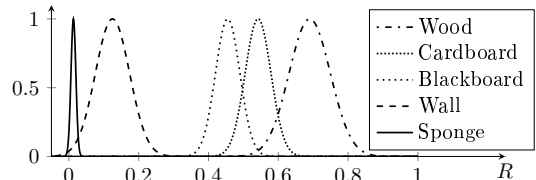


Figure 6: The dispersion of the reflection coefficient R for different materials.

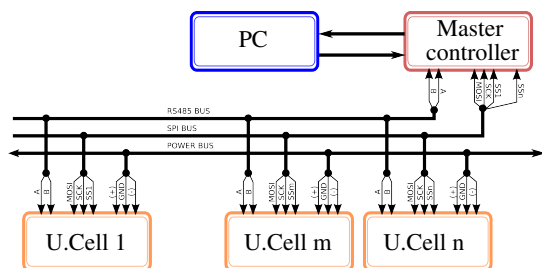


Figure 7: The topology of the distributed sensory system.

is connected with the PC using both USB and RS485 bus. In theory, based on the number of available pins, this controller can program up to 50 ultrasonic cells.

In order to control, optionally (re)program and power the ultrasonic cells, a hybrid 8-pin bus was used. It consists from: 1. communication bus based on RS-485 standard (2 pins), 2. programming bus which uses SPI communication (3 pins), and 3. the power line provided from a bipolar 10-15V power supply (3 pins). It is interesting that in order to use standard 8-pin Ethernet connectors and cables, the MISO line is excluded from the SPI bus, therefore reducing the needed number of wires from 9 to 8. This means that cell programming is executed "blindly", and that the reprogrammed cell itself must report that it is successfully programmed. In case of any malfunction, the user may use the ICSP connectors equipped with 4 pin SPI bus directly available on the ultrasonic cell PCB.

3.3 Software on PC

In order to effectively control and test the ultrasonic cell array, a suitable software application needed to be developed. Currently, the graphical user interface (GUI) of the developed application in MATLAB is not finished nor fully interactive. However, most of the 1D visualisation functions, definitions and dispositions of sensors, real-time communication with remote ultrasonic cells, replication of obstacles and simple data fusion are implemented as scripts and accessible using command line. Screenshots from implemented measurement indications are shown in Figures 10 and 11.

4 EXPERIMENTAL SETUP AND DISCUSSION

In this paper we will focus on discussing a part of experimentally obtained data using the designed 1D ultrasonic ultrasonic array (with up to 8 sensors), and

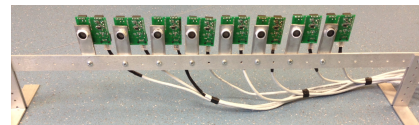


Figure 8: Physical disposition of an ultrasonic array - linear mode.



Figure 9: Physical disposition of an ultrasonic array - circular mode.

pinpoint the advantages and drawbacks of the designed system.

In order to test the functionality of the system, the ultrasonic cells are spatially aligned into two typical dispositions: linear (Figure 8) and circular (Figure 9).

Sick LMS220 Laser system was used for verification of the measurement results, as well as image fusion. It has angular resolution up to 0.25 degree, although the measurement are re-sampled with 2 degrees resolution for easier view. The laser connects directly to the master PC via USB/RS232 converter.

4.1 Linear Sensor Disposition

Figure 10 depicts one interesting demonstration setup, where sensors are distributed 10cm apart on a straight line parallel to a two material obstacle (wood and plasterboard). Despite their significant directivity and very narrow beam angles (around 3 to 5 degrees), each sensor is able to relatively accurately detect the presence and distance of the obstacle set around 80cm from the sensors. In addition, they provide the reflection coefficients of their sensed obstacle, which is computed using the distance of the obstacle and the magnitude of the reflected signal (Equation (4)).

For viewing purpose, the measurement (distance, reflection coefficient)=(d_i, R_i) of i -th sensor ($i = 1, \dots, 8$) positioned at location (x_i, y_i) is visually presented using the following rules:

- each measurement d_i is marked with a circle C_i positioned at location (x_i, d_i) ,
- the circle C_i is shaded using the value R_i (zero means completely acoustically absorptive, and one means completely reflexive surface)

- the thick segments that connect circles C_i and C_{i+1} are given in parametric form $x = (1-t)x_i + tx_{i+1}$ and $y = (1-t)d_i + td_{i+1}$, and shaded using the function $r(t) = R_i(1-t) + R_{i+1}t$ where $0 \leq t \leq 1$,
- if the measurements obtained from ultrasound or lasers are out of figure viewing range, the measurement are clipped for simpler representation.

It is visible from Figure 10 that ultrasonic sensors readings are quite informative and provide a very similar representation of the actual scenario. The obstacle is visible and its left and right side are represented by different reflection coefficients, therefore they may indicate different materials. This type of information may be of significant importance for an autonomous robotic system (e.g. parking sensors, navigation and mapping, material inspection etc.).

4.2 Circular Sensor Disposition

Another specific experiment is demonstrated in Figure 11. The sensors are spatially distributed on a semi-circle, 25 degrees apart. A solid wooden obstacle is positioned at the same distance as in the first experiment (80cm from the laser).

Due to the relatively poor angular resolution of the sensor array, in cases such as one depicted on Figure 11 it is possible that only a small number of sensors detect the obstacle. Nevertheless, using data fusion of ultrasonic readings with laser reading, the obtained results may be used to enrich the visual representation of laser readings only. The principal idea is to map sensor readings onto the laser measured contour. The algorithm is formulated similarly to the case of linearly arranged sensors:

- each measurement d_i from sensor positioned at (x_i, y_i) and rotated for α_i is marked with a circle C_i positioned at location $(x_i + d_i \cos(\alpha_i), y_i + d_i \sin(\alpha_i)) = (xL_i, yL_i)$,
- the circle C_i is shaded using the value R_i ,
- for each of the measurements from the laser (angle,distance)= (β_j, d_j) where $j = 1 \dots (\text{max.laser.angle/ang.resolution})$, sets of corresponding indices i and j are found such that $|\alpha_i - \beta_j|$ is minimal. The latter set shall be denoted as $J = \{j_1, j_2, \dots, j_n\}$ where n is the number of used sensors.
- for each part of the laser obtained contour which lies between points j_k and j_{k+1} where $k = 1, \dots, n$ (in total $s = j_{k+1} - j_k$ number of segments), every smaller segment $< j_p, j_{p+1} >$ is drawn by a thick line and linearly shaded using the interpolation $r(t) = R_{j_p}(1-t) + R_{j_{p+1}}t = (R_{j_k} + ((p -$

$$k)/s) * (R(j_{k+1}) - R(j_k))(1-t) + (R_{j_k} + ((p - k + 1)/s) * (R(j_{k+1}) - R(j_k))t \text{ where } 0 \leq t \leq 1,$$

- if the measurements obtained from ultrasound or lasers are out of figure viewing range, the measurement are clipped for simpler representation.

The visual interpretation of fused laser and ultrasonic data derived using the latter algorithm are presented in Figure 11.

4.3 Discussion and Guidelines for Future Work

The system proposed hybrid ultrasound-based sensory has great potential for creating informationally rich images of the environment, especially when differentiating surfaces or structure of objects. Nevertheless, additional improvements need to be made.

As for the hardware, the burst length, amplification levels and calibration of ultrasonic cells needs to be investigated more thoroughly. Additional mechanisms that allow motions of the sensor platform, in combination with a suitable algorithm which exploits the possibility of "single cell sender - multiple cells receivers" concept would certainly compensate the drawbacks of ultrasonic cells (such as directivity). Moreover, adding horns to sensors would change the amplification and directivity of the cells.

The visualisation software needs to be improved, in order to allow easy user interaction (adding sensors, obstacles, display measurements etc.). In addition, the RGB camera readings and readings from a 2D ultrasonic array needs to be fused.

ACKNOWLEDGEMENTS

This research is conducted as part of the project "A hybrid 2D visualization of the environment using ultrasonic reflections", funded by the Federal Ministry of Education and Science Bosnia and Herzegovina.

REFERENCES

- Benet, G., Blanes, F., Simó, J. E., and Pérez, P. (2002). Using infrared sensors for distance measurement in mobile robots. *Robotics and autonomous systems*, 40(4):255–266.
- D. Champaigne, Kevin andSumners, J. (2007). Low-power electronics for distributed impact detection and piezoelectric sensor applications. *Aerospace Conference*, 9:3911–3919.
- Elfes, A., M. Dolan, J., Podnar, G., Mau, S., and Marcel, B. (2006). On generating the motion of industrial

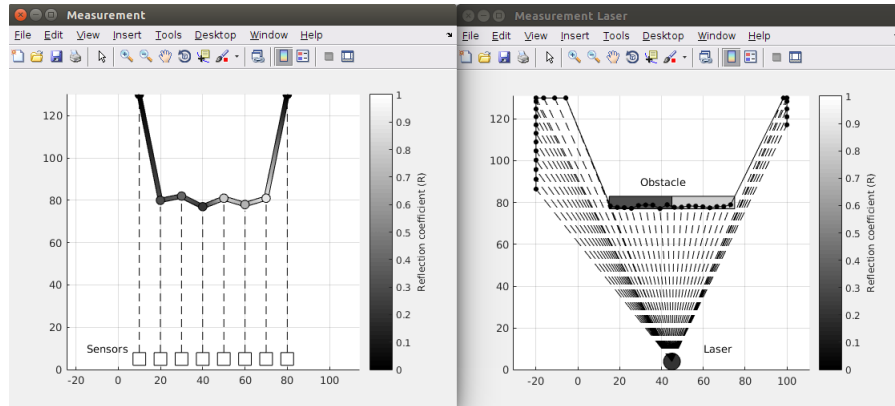


Figure 10: Left: visualisation of measurement results obtained by linearly positioned ultrasonic cells, Right: visualisation of laser measurements and presentation of the actual obstacle. Different grayscale tones are used for depicting the determined reflection coefficient.

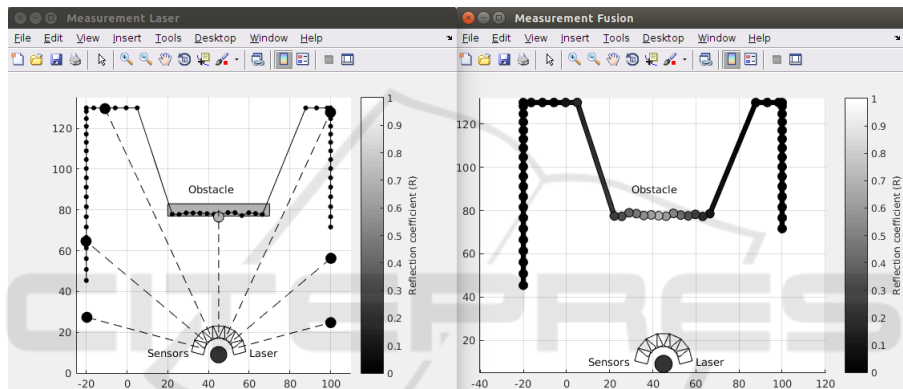


Figure 11: Left: visualisation of measurement results obtained by circularly positioned ultrasonic cells, laser measurements and reconstruction of actual obstacle. Right: Fusion of laser and ultrasonic data. Different grayscale tones are used for depicting the extrapolated reflection coefficient.

- robot manipulators. *Safe and efficient robotic space exploration with tele-supervised autonomous robots*, 1:104–113.
- Fernández, I., Mazo, M., Lázaro, J. L., Pizarro, D., Santiso, E., Martín, P., and Losada, C. (2007). Guidance of a mobile robot using an array of static cameras located in the environment. *Autonomous Robots*, 23(4):305–324.
- Fuentes-Pacheco, J., Ruiz-Ascencio, J., and Rendón-Mancha, J. M. (2015). Visual simultaneous localization and mapping: a survey. *Artificial Intelligence Review*, 43(1):55–81.
- Grzelak, S., Czoków, J., Kowalski, M., and Zieliński, M. (2014). Ultrasonic flow measurement with high resolution. *Metrology and Measurement Systems*, 21(2):305–316.
- Han, X., Wang, J., Peng, Z., and Zhang, J. (2011). A study of ultrasonic flowmeter in ship piping leakage detection system. *Intelligent Systems and applications (ISA)*, 1:769–773.
- Jung, H. G., Cho, Y. H., Yoon, P. J., and Kim, J. (2008). Scanning laser radar-based target position designation for parking aid system. *Intelligent Transportation Systems, IEEE Transactions on*, 9(3):406–424.
- Kaltsoukalas, K., Makris, S., and Chryssolouris, G. (2015). On generating the motion of industrial robot manipulators. *Robotics and Computer-Integrated Manufacturing*, 32:65–71.
- Kim, D.-H., Yang, B.-S., and Lee, S.-B. (2011). 3d boiler tube leak detection technique using acoustic emission signals for power plant structure health monitoring. *Prognostics and System Health Management Conference*, 1:256–263.
- Vladišauskas, A. and Jakevičius, L. (2004). Absorption of ultrasonic waves in air. *Ultragarsas*, 1:50.
- Ye, P.-x. and Song, Z.-j. (2012). Truncation and aliasing errors for Whittaker-Kotelnikov-Shannon sampling expansion. *Applied Mathematics-A Journal of Chinese Universities*, 27(4):412–418.
- Zubaca, J., Ferizbegovic, M., Softic, K., Sokic, E., and Ahic-Djokic, M. (2015). Design of a distributed ultrasound-based sensory system. In *Information, Communication and Automation Technologies (ICAT), 2015 XXV International Conference on*, pages 1–6. IEEE.